Measurement of interaction forces between fibrinogen coated probes and mica surface with the atomic force microscope: The *p*H and ionic strength effect

Theodora S. Tsapikouni
Laboratory of Biomechanics and Biomedical Engineering, Mechanical Engineering and Aeronautics Department, University of Patras, Patras, 26504, Greece

Stephanie Allen
Laboratory of Biophysics and Surface Analysis, School of Pharmacy, Boots Science Building, The University of Nottingham, University Park, Nottingham, NG7 2RD, United Kingdom

Yannis F. Missirlis[a)]
Laboratory of Biomechanics and Biomedical Engineering, Mechanical Engineering and Aeronautics Department, University of Patras, Patras, 26504, Greece

(Received 23 October 2007; accepted 8 January 2008; published 21 February 2008)

The study of protein-surface interactions is of great significance in the design of biomaterials and the evaluation of molecular processes in tissue engineering. The authors have used atomic force microscopy (AFM) to directly measure the force of attraction/adhesion of fibrinogen coated tips to mica surfaces and reveal the effect of the surrounding solution *p*H and ionic strength on this interaction. Silica colloid spheres were attached to the AFM cantilevers and, after plasma deposition of poly(acrylic acid), fibrinogen molecules were covalently bound on them with the help of the cross-linker 1-ethyl-3-(3-dimethylaminopropyl) carbodiimide hydrochloride (EDC) in the presence of N-hydroxysulfosuccinimide (sulfo-NHS). The measurements suggest that fibrinogen adsorption is controlled by the screening of electrostatic repulsion as the salt concentration increases from 15 to 150 mM, whereas at higher ionic strength (500 mM) the hydration forces and the compact molecular conformation become crucial, restricting adsorption. The protein attraction to the surface increases at the isoelectric point of fibrinogen (*p*H 5.8), compared with the physiological *p*H. At *p*H 3.5, apart from fibrinogen attraction to the surface, evidence of fibrinogen conformational changes is observed, as the *p*H and the ionic strength are set back and forth, and these changes may account for fibrinogen aggregation in the protein solution at this *p*H. © *2008 American Vacuum Society.* [DOI: 10.1116/1.2840052]

I. INTRODUCTION

Knowing the details of protein adsorption, although essential for biomaterials design, is quite a difficult task, since the adsorption process is controlled by various enthalpic and entropic processes. Enthalpic contributions stem from van der Waals forces, the overlap of electrical double layers, and hydrophobic interactions,[1] while entropic mechanisms involve dehydration of hydrophobic regions, conformational changes of the protein, and release after adsorption of co-adsorbed ions in the layer separating protein and substrate.[2] It is obvious that protein adsorption depends on the charge distribution in both the specimen and the substrate as well as on the counterions in the adsorption solution.[3] Variations of the *p*H and the ionic strength could then regulate the adsorption driving forces and contribute to an understanding of their competitive role.

Several investigations of the effect of *p*H and ionic strength on protein adsorption have been reported in the literature: conformational differences have been observed with scanning electron microscopy[4,5] and retained protein mass has been quantified with spectophotometry,[6] neutron reflection,[7] fluorescence spectroscopy,[8] or ellipsometry.[9] The invention and the widespread of the use of atomic force microscopy (AFM) initiated further a series of direct and accurate measurements of the interaction forces between modified tips and surfaces[10–15] and this technique was soon exploited for the study of the influence of *p*H and ionic strength on the interaction between adsorbed protein layers.[16–19]

Atomic force spectroscopy is based on recording the deflection of a very sensitive cantilever, while it is approaching or being retracted from a surface. Deflection measurements can be easily transformed into force data using the spring constant of the cantilever and displayed as the relative probe-surface separation distance. In cases where the measurement of the interaction between adsorbed protein layers is desired, the AFM probe is usually first modified with a micrometer-sized sphere.[20,21] Attaching a colloid sphere to the cantilever helps overcome the problems due to variable tip geometry or sample coating inconsistencies and inhomogeneities. Besides, the larger radius, compared with that of a bare tip, allows smaller forces to be detected with higher sensitivity.[22] It should be mentioned, however, that the lateral resolution is reduced to a few micrometers.

[a)]Author to whom correspondence should be addressed; electronic mail: misirlis@mech.upatras.gr

We have used such modified AFM probes to measure the interaction force between fibrinogen molecules, covalently bound on the colloid sphere, and mica surfaces at various *p*H and ionic strength conditions. For such experiments covalent binding is preferable over physi-sorption, because it assures stronger immobilization of the molecules to the sphere than the interfacial force being measured,[3,23] and averts any misinterpretation of the measured detachment force. Following the hypothesis of Meagher *et al.*,[19] we assume that the surface behavior of the immobilized fibrinogen layer reflects that of the protein in solution. When using a nonselective attachment method, via the lysine or primary amine groups, for example, the molecules may not be bound on the sphere in a unique orientation and, although they may expose inner epitopes after the immobilization, the measured forces can give an estimation of the average interaction of the protein in the solution with the surface. Moreover, it should be pointed out that protein adsorption on a surface is not directly related to the adhesion force. However, evidence[20] shows that there can be correlation between these two parameters.

Following this argument it is reasonable to juxtapose the protein-surface interaction forces, recorded in this set of experiments, with the results of our previous work.[24] In that study, AFM images of single fibrinogen molecules, adsorbed onto mica surfaces from buffers of different *p*H's and ionic strengths, were obtained and the surface coverage calculated in order to demonstrate the effect of solution conditions on protein adsorption.

Fibrinogen has been the object of both studies due to its significant role in plasma. Revealing the forces, which enhance or prevent its adsorption, will shed light into the mechanisms of the Vroman effect,[25] explain the adsorption-induced polymerization into fibrin on surfaces,[26] and, finally, help estimate the viability of prosthetic biomaterials.

II. MATERIALS AND METHODS

A. Preparation of colloid probes

Triangular, 200-μm-long, narrow legged Si_3N_4 cantilevers (NP-S, Veeco Probes, Camarillo, CA, USA) were modified with single silica spheres (4.9 ± 0.5 μm diameter, Duke Scientific Corporation, Fremont, CA). Prior to modification the probes were washed with acetone and their spring constants individually calibrated using the thermal method.[27,28] An average value of 0.078 ± 0.008 N/m was calculated for a batch of 16 cantilevers with 0.06 N/m nominal spring constant. The colloid spheres were then attached to the cantilevers with Araldite Rapid Resin using the stage and the head of a Multimode AFM (Digital Instruments, Veeco, Santa Barbara, CA) as a micromanipulator. The attachment was confirmed by images obtained with a scanning electron microscope (Jeol JSM-6060, Japan) at 20 keV and 2400× magnification.

B. Chemical modification of the colloid probes

The colloid probes were etched in an O_2 plasma for 5 min in a custom built plasma chamber and then coated with plasma polymerized acrylic acid.[29] For the deposition, the chamber was first pumped down to 25 mTorr and then acrylic acid vapor (Sigma-Aldrich, Dorset, U.K.), previously submitted to a freeze-pump-thaw cycle, was let in, until the pressure was stabilized at 300 mTorr. The power was turned on and set to 20 W for the time needed until a final polymer thickness of 40 nm was indicated by the quartz crystal microbalance fitted in the chamber. The modified probes were kept under vacuum in a desiccator until they were used. To check the plasma process, mica samples as well as glass coverslips (previously cleaned with piranha solution) were modified in parallel. These were used for AFM imaging with a Nanoscope IIIa Multimode (Digital Intruments, Veeco, Santa Barbara, CA) and contact angle measurements (Cam 200, KSV Inc., Helsinki, Finland).

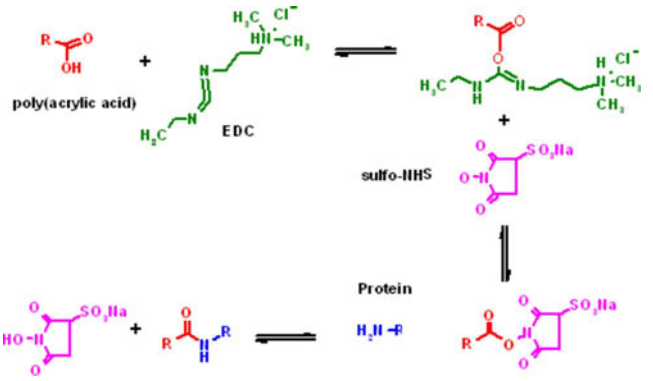

FIG. 1. Amide bond formation between poly(acrylic acid) and fibrinogen molecules through esterification with EDC in the presence of sulfo-NHS.

C. Functionalization with fibrinogen

Fibrinogen molecules were covalently bound to the colloid probes after activation of the carboxyl groups on the surface of the poly(acrylic acid) with 1-ethyl-3-(3-dimethylaminopropyl)-carbodiimide hydrochloride (EDC, Sigma Aldrich, Dorset, U.K.) and N-hydroxysulfosuccinimide (sulfo-NHS, Fluka, Dorset, U.K.) (Fig. 1). Sulfo-NHS is added in order to increase the stability of the ester intermediate, O-acylisourea, which otherwise would strongly hydrolyze, regenerating the carboxylate group. For the esterification reaction, the probes were immersed in PBS solution containing 6 mM EDC and 15 mM sulfo-NHS for 15 min. The *p*H of the reaction buffer was set to 6 in order to slow down the hydrolysis of the active ester formed.[30] After rinsing with PBS, they were immersed in a 10 μg/ml fibrinogen solution (PBS *p*H 7.4) for 2 h, so that protein molecules could be immobilized on the surface of the colloid sphere by forming peptide bonds via their amino groups. Lyophilized fibrinogen was purchased from Sigma-Aldrich and used without further purification.

D. Force measurements

The measurements of the interaction force between the functionalized probes and freshly cleaved mica surfaces were

carried out with a 1D molecular force probe (MFP-1D, Asylum Research, Santa Barbara, CA). Force curves were recorded in five different buffered solutions: 5 mM phosphate buffer was regulated with NaCl up to 15, 150, or 500 mM for varying ionic strength, at *p*H 7.4, or adjusted at *p*H 3.5, 5.8, or 7.4 for varying *p*H, at 150 mM ionic strength. The frequency of the approach/retraction cycle was 1 Hz and the velocity was approximately 800 nm/s. The measurements were repeated with five different tips and at least 100 curves were collected with each tip at each ionic strength or *p*H. The solutions were exchanged in random order to check for any irreversible effect on the adsorbed protein layer. Attention was also paid to ensure that the maximum force applied upon compression of the probe onto the surface did not to exceed 800 pN.

III. RESULTS AND DISCUSSION

A. Probe modification

Deposition of plasma polymerized poly(acrylic acid) on the colloid probes was first examined by modification of mica and glass samples. Contact angle measurements acquired immediately after the plasma deposition showed an increase of contact angle on both substrates [$79 \pm 9.6°$ from $3 \pm 1.2°$ on mica, and $67 \pm 5.0°$ from $22 \pm 1.6°$ on glass coverslips (average values over three samples)]. The relatively high contact angles of poly(acrylic acid) plasma coatings may be attributed to the extensive fragmentation of the starting monomer due to the high power used to assure crosslinking.[31] However, after 1 h incubation in PBS and drying under N_2, the wettability of mica returned to the pre-plasma-treatment levels, whereas glass coverslips retained their acquired hydrophobicity.

AFM images of both materials in air displayed a granular topography, with surface features not higher than 4 nm, indicative of the polymer deposition [Figs. 2(a) and 2(b)]. Images acquired in PBS, however, showed that mica substrates regained their initial featureless and smooth appearance [Fig. 2(c)]. In contrast, the glass substrate showed a moderate swelling [Fig. 2(d)]. These observations may lead to the conclusion that poly(acrylic acid) is not strongly cross-linked on the mica surface under the processing conditions used here[31] and dissolves away in the water solution, for which the cation exchange on the cleaved mica surface might also be responsible.[32,33] Nonetheless, it has been shown that the glass coverslips can be effectively coated with the polymer. This enabled us to proceed with the functionalization of the silica colloid probes with fibrinogen considering, at the same time, any compressibility effects of the swelled polymer layer.

Interaction forces between the colloid probes and bare mica surfaces were recorded at both modification steps, i.e., after plasma deposition and after fibrinogen covalent binding with EDC and sulfo-NHS, to ensure that the spheres had been indeed functionalized with the protein and the measured forces result from the protein layer, and not the polymer, interacting with the surface. All the curves recorded

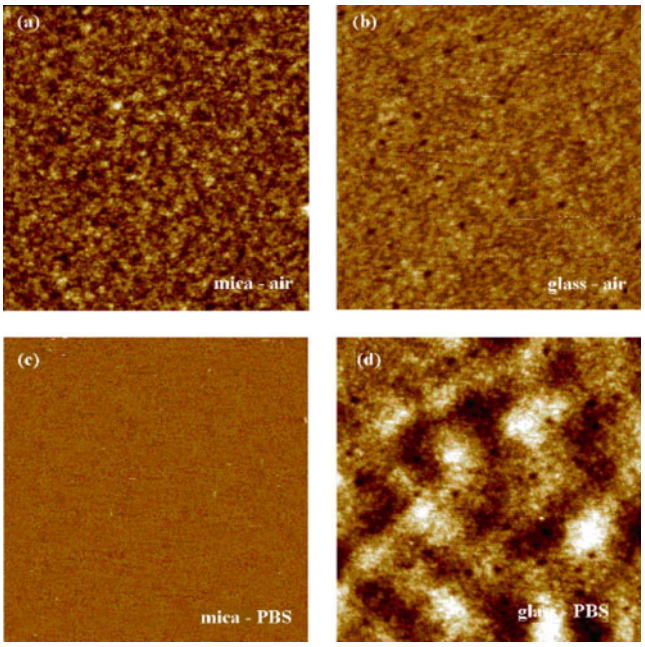

FIG. 2. AFM images of plasma deposited poly(acrylic acid) on mica (a) and glass (b) in air. After immersion in PBS the polymer layer was washed from the mica surface (c), whereas it was swollen on the glass coverslip (d). All images were obtained with tapping mode (c and d in PBS), lateral scan size 1×1 μm^2, z range 5 nm.

with the plasma treated probes indicated no adhesion upon retraction [Fig. 3(a)]. In contrast, the curves derived by using the fibrinogen-functionalized probes show detachment of the protein molecules from the surface, either as individuals or as part of a film [Fig. 3(b)]. The possibility of concurrently stretching the protein and/or the underlying polymer layer cannot be excluded; however, it does not compromise the observed detachment event. Moreover. the polymer properties may contribute to the *p*H or ionic strength dependence of the probe interaction with the surface, but this effect must be limited because the majority of the charged groups on it, the carboxylic acids, are thought to be coupled with protein residues.

B. Force profiles upon approach with variation in ionic strength

Figure 4(a) shows representative force curves recorded upon approach of a fibrinogen-coated probe to the mica surface in PBS (*p*H 7.4) at various ionic strengths. At 15 mM the force profile reveals repulsion at tip-surface separations smaller than 10 nm, assuming that the protein-solution interface lays at 6 nm (see below). This can be attributed to the electrostatic force between the protein layer and the mica, which is repulsive, for they are both negatively charged at *p*H 7.4.[34] As the ionic strength is increased to 150 mM, the probe is no longer repelled from the surface, but it is attracted by it. The increase of the NaCl concentration results in the reduction of the thickness of the diffusive double layers in both the protein layer and the mica surface,[35] so that the electrostatic repulsion is restricted in range and the van

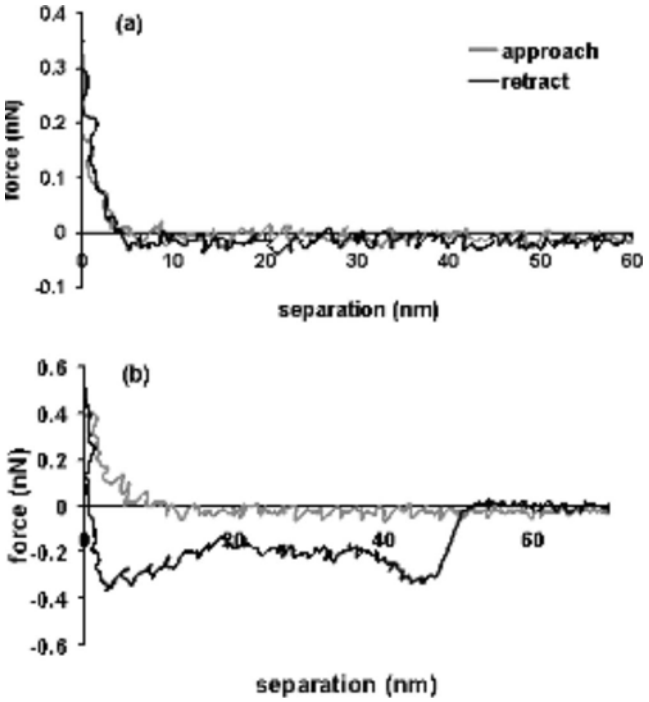

FIG. 3. Force curves collected upon approach (gray line) or retract (black line) of (a) a poly(acrylic acid)-coated probe and (b) a fibrinogen-coated probe, from a mica surface in 15 mM PBS (*p*H 7.4). The plasma treated probes indicate no adhesion upon retraction in contrast to the fibrinogen-functionalized probes, which reveal unfolding of the protein molecules and/or the underlying polymer layer before detachment.

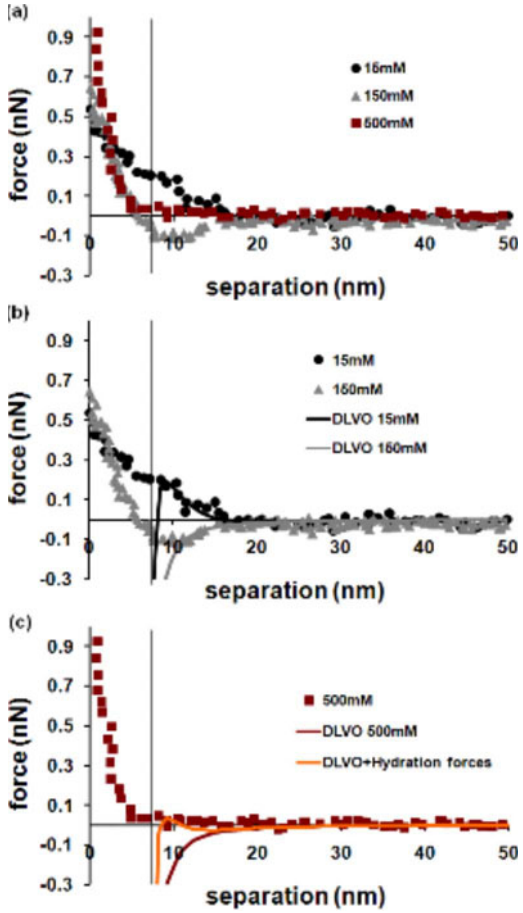

FIG. 4. (a) Interaction force vs separation, as measured upon approach of a fibrinogen coated probe to mica surface in 15 (●),150 (▲), and 500 mM (■) PBS (*p*H 7.4). (b) Theoretical curves, derived from the DLVO model, Eq. (3), fit the experimental curves: black line for 15 mM, gray line for 150 mM. (c) Fitting curve according to the same model for 500 mM (red line). Incorporation of the hydration term in Eq. (4) provided a better fit for the higher ionic strength (orange line). The vertical line is set at the protein-solution interface, i.e., at 6 nm. The experimental data have been fitted up to this distance, since beyond it the DLVO model is invalid due to the strong steric repulsions.

der Waals attraction becomes dominant at small probe-surface separation distances. The dominance of van der Waals forces is not, however, maintained when the ionic strength is further increased. At 500 mM neither repulsion nor attraction is recorded as the probe is approaching the surface.

There seems to be close agreement between the force profiles, recorded at the three ionic strengths, and the measurements of surface coverage of single fibrinogen molecules on the mica surface, quoted in our previous work.[24] We had found that fibrinogen adsorption is enhanced as the ionic strength is raised from 15 to 150 mM, an observation which is now justified by the conversion of the protein-surface interaction force from repulsive at 15 mM to attractive at 150 mM. At 500 mM the surface coverage was decreased and this reduction, which could not be explained by the double layer theory, was indirectly accounted for by the reduction of the effective protein concentration due to aggregation. The force measurements have supplied a more straightforward reasoning: no attraction is recorded any more between the protein and the surface. But the origin of the repulsive protein-surface interaction force, which shields the van der Waals attraction, has to be investigated.

Enhancement of steric repulsion[19,36] at the higher salt concentration should not be expected, since screening of intra- and intermolecular repulsions results in a more compact conformation of the protein molecules on the bound layer.[17] Therefore, steric interactions cannot be responsible for the force profile at the 500 mM. On the other hand, repulsive hydration forces between negatively charged surfaces may become significant at high salt concentrations, because of the high number of hydrated Na^+ ions trapped between them.[37] We have checked if this speculation applies in our case by fitting the DLVO (Derjaguin–Landau–Verwey–Overbeek) model to the experimental curves and incorporating an additional hydration term for the higher ionic strength.

The DLVO theory[38] describes the interaction between two surfaces as a combination of electrostatic and van der Waals forces.[39] According to the boundary conditions taken into account, either of constant surface charge or constant surface potential, two solutions of the Poisson-Boltzmann equation can arise.[40] The real interaction force will lie between these two limits and likely closer to the constant-potential solution.[18,19] An approximate expression can be otherwise used at low surface potentials (<25 mV) and provide results, which compare well to the solution of the constant

potential boundary conditions. For the interaction between the AFM probe and the mica surface this expression takes the form of the following equation:[22,41]

$$F = F_{\text{elect}} + F_{\text{vdWaals}} = \frac{4\pi\sigma_S\sigma_P R\lambda}{\varepsilon\varepsilon_o} e^{-x/\lambda} - \frac{AR}{6x^2}, \quad (1)$$

with σ_P and σ_S being the surface charge densities of the probe and the surface, respectively, ε_o being the permittivity of the vacuum, ε being the dielectric constant of the medium, R being the colloid sphere radius, A being the Hamaker constant, x being the probe-surface separation, and λ being the Debye length. The Debye length is a measure of the thickness of the diffusive electric double layer and correlates the ionic strength of the solution with the interaction forces according to the equation

$$\lambda = \sqrt{\frac{\varepsilon\varepsilon_o kT}{e^2 \sum_i c_i q_i^2}}, \quad (2)$$

where k is the Boltzmann constant, T is the absolute temperature, e is the electron charge, q_i is the ionic valency, and c_i is the concentration of the ith electrolyte component in the solution.

The force versus separation experimental curves have been positioned using the point of "hard wall contact" as the point of zero separation, i.e., the point at which the substrate and the probe start to move jointly. However, the probe-surface contact may initiate earlier and a reasonable estimation of the distance due to the compression of the polymer-protein layer on the colloid sphere can be drawn from the point of first contact at the 150 mM curve [Fig. 4(a)], which occurs at around 6 nm. For the rest of the analysis, the protein-solution interface is assumed to lay 6 nm away from the compliance plane and this interface is regarded as the plane of origin of the DLVO forces, since beyond this point the steric repulsions become significant. Therefore, the variable x in Eq. (1) is replaced by the variable $x' = x - d$, where $d = 6$ nm and Eq. (1) is transformed to

$$F = F_{\text{elect}} + F_{\text{vdwaals}} = \frac{4\pi\sigma_S\sigma_P R\lambda}{\varepsilon\varepsilon_o} e^{-(x-d)/\lambda} - \frac{AR}{6(x-d)^2}. \quad (3)$$

The Hamaker constant has been assigned[18] the value 7.5×10^{-21} J (Ref. 18) and the σ_P, σ_S parameters have been optimized through the experimental data fitting using as initial inputs values suggested in the literature.[19,35] It should be underlined that as the ionic strength is increased the surface charges of the mica and the protein layer remain constant and equal to -0.0046 and -0.0035 C/m^2, respectively.

The resultant theoretical curves are displayed in Figs. 4(a) and 4(b). The experimental data have been fitted up to the protein-solution interface, i.e., up to 6 nm separation. At the two lower ionic strengths (15 and 150 mM) the theoretical curves are closely fitted to the experimental data, although at very small separations the AFM cantilever cannot follow the deep attraction well due to its finite stiffness.[42] At the 500 mM the DLVO model fails to describe the protein-surface interaction. We thus rewrite Eq. (3) including an exponential term, which describes the hydration force,[40] so that the expression of the interaction force becomes

$$F = F_{\text{elect}} + F_{\text{vdWaals}} + F_{\text{hydr}} = \frac{4\pi\sigma_S\sigma_P R\lambda}{\varepsilon\varepsilon_o} e^{-(x-d)/\lambda} - \frac{AR}{6(x-d)^2} + C_H \,\text{Re}^{-(x-d)/\kappa}, \quad (4)$$

where C_H is an empirical hydration constant and κ is the hydration force decay length.

The experimental data at 500 mM can now be closely fitted by Eq. (4) [Fig. 4(c)]. The values assigned to the C_H and κ fitting parameters (0.8 mN/m and 1.8 nm, respectively) are close to the ranges suggested in the literature, although the decay length seems to be rather large, when compared with the hydration radius of the Na^+ cations, which is 0.36 nm.[40] Protrusion of the protein molecules may be responsible for the extended range of the hydration repulsion.[16] Steric repulsions can be one reason for divergence between the experimental and the theoretical curves, at separations smaller than 2 nm, whether or not the hydration term is included, but there may be more reasons. The Hamaker constant at such separations is likely different than that determined for the bulk solution because of retardation phenomena or squeezing of cations between the two surfaces. However, the differences should not be significant and the power of the theoretical model to describe the measured forces at larger separations is not diminished, as it is otherwise proved by Fig. 4(c).

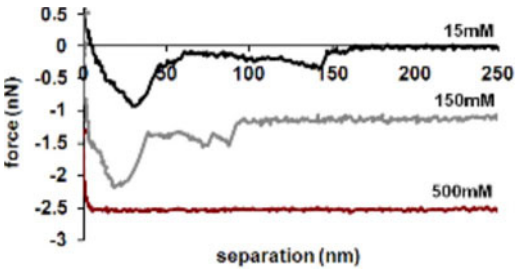

FIG. 5. Force curves collected upon retraction of a fibrinogen coated probe from mica surface in 15, 150, and 500 mM PBS, adjusted with NaCl (pH 7.4). Protein adhesion to the mica surface, present at the two lower ionic strengths, disappears at 500 mM. The curves have been shifted vertically for clarity.

C. Detachment forces at different ionic strengths

To further investigate the ionic strength effect on fibrinogen interaction with surfaces, the retract traces of the force curves recorded in the above experiment were analyzed. Figure 5 shows one representative retraction curve for each salt concentration. At 15 and 150 mM detachment forces of approximately 1 nN were recorded whereas at 500 mM no adhesion to the substrate was found to occur. The elimination of protein-surface adhesion was systematically observed whenever the salt concentration was raised to 500 mM, irrespective of the sequence of the changes in pH or ionic strength, with one exception (pH 3.5) to be discussed later. These observations imply that at the highest salt concentra-

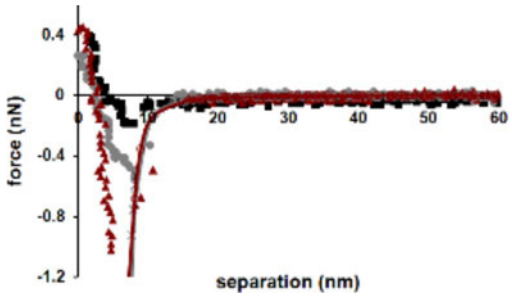

FIG. 6. Interaction force vs separation upon approach of a fibrinogen coated probe to mica surface in 150 mM PBS at *p*H 7.4 (■), 5.8 (●), and 3.5 (▲). The continuous lines represent fitting curves according to the DLVO model, Eq. (3), and the fitting parameters listed in Table I [(⟠) for *p*H 7.4, (⨯) for *p*H 5.8, and (⊖) for *p*H 3.5].

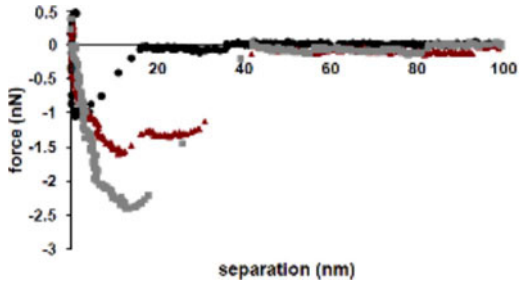

FIG. 7. Force curves collected upon retraction of a fibrinogen coated probe from mica surface in 150 mM PBS at *p*H 7.4 (●), 5.8 (▲), and 3.5 (■).

tion, where the electrostatic repulsions between the protein residues are screened,[4,43] fibrinogen obtains a compact conformation, which prevents it from forming adhesive bonds with the mica surface. A similar effect was reported by Zhang *et al.*,[16] who observed a decrease in vitronectin intermolecular adhesion force as the NaCl concentration was increased. We may conclude then that an excessive increase of salt in the protein solution inhibits adsorption not only via the hydration forces but also by altering the natural protein conformation and blocking binding sites.

It is important to note that the measured detachment forces do not reflect the long-term adsorption behavior, since the encounter time of the probe with the surface was of the order of tens of ms. Increased encounter times could probably reveal conformational adaptations of the protein on the surface.[44]

D. Influence of *p*H

The fibrinogen-surface interaction as a function of solution *p*H was investigated by recording force curves at *p*H 7.4, 5.8, and 3.5 while keeping the solution ionic strength constant at 150 mM. Due to the screening of the electrostatic forces at this salt concentration, which is close to that which occurs in physiological environments,[45] the DLVO model does not predict any significant difference in the approaching curves at the three *p*H's. The theoretical curves, drawn in Fig. 6, according to the surface charge values listed in Table I, almost overlap. The experimental data, on the other hand, revealed stronger attraction of the colloid probe to the surface at *p*H 5.8 and 3.5, compared with the physiological one, at separations smaller than 10 nm (Fig. 6). At *p*H 5.8, which is the isoelectric point (iep) of fibrinogen, and at *p*H 3.5, which is close to the iep of mica,[46] the interaction is expected to be more attractive than at *p*H 7.4. However, as it has been shown, the electrostatic forces are screened at the salt concentration used in this set of measurements, i.e., at 150 mM [Fig. 4(a)], and so their effect on probe-surface interaction is limited. We make the assumption, then, that hydration forces may again be responsible for the differences observed. Although not taken into consideration previously, when fitting the experimental curve at *p*H 7.4 and 150 mM with the DLVO formula, a slightly increased Na^+ concentration should be present at the neutral *p*H, compared with the lower *p*H's, resulting in an osmotic pressure repulsion and partial shielding of the van der Waals attraction. As the *p*H becomes more acidic and both surfaces are neutralized or get positively charged, hydration forces lose their significance, since the Cl^- counterions are very weakly solvated ions.[40] As a result, the van der Waals attraction, possibly supported by the weak electrostatic attraction, appears in the experimental force curves.

We cannot, nevertheless, exclude the possibility that the theoretical curves fail to describe the experimental ones, because the former do not include an attractive electrostatic contribution.[47,48] Such attraction occurs at small separations due to the surface charge reversion as ions are pushed back to the surfaces, since the surface potentials are assumed constant. This could be particularly true at *p*H 5.8 and 3.4, because at this *p*H the mica and the protein layer surfaces are less charged and thus the charge reversal is more probable.

The stronger attraction of the fibrinogen coated probe to the mica surface at *p*H 3.5 is in contradiction to our previous measurements of surface coverage of fibrinogen molecules, which showed a dramatic decrease of adsorption at the same *p*H.[24] In that study we also noticed some aggregates on the mica surface and then made the assumption that at *p*H 3.5 conformational changes, which result in protein aggregation, may occur. We tried to confirm this speculation by recording the protein adhesion to the surface, while the colloid probe was being withdrawn at the different *p*H's. Such retraction curves show strong detachment forces at all the *p*H's studied (Fig. 7). However, a rather interesting effect was observed when the conditions of the measurement buffer were changed in the following order: from 500 mM at *p*H 7.4 to 150 mM at *p*H 3.5 and then back to 500 mM at *p*H 7.4.

TABLE I. Adjusted surface charge of mica (σ_S) and fibrinogen layer (σ_P) for the fitting of the theoretical DLVO equation to the experimental curves at different *p*H's at 150 mM ionic strength.

		*p*H 7.4	*p*H 5.8 (iep of fibrinogen)	*p*H 3.5 (iep of mica)
150 mM	σ_P=	−0.0035 C/m^2	0 C/m^2	0.005 C/m^2
	σ_S=	−0.0046 C/m^2	−0.002 C/m^2	−0.001 C/m^2

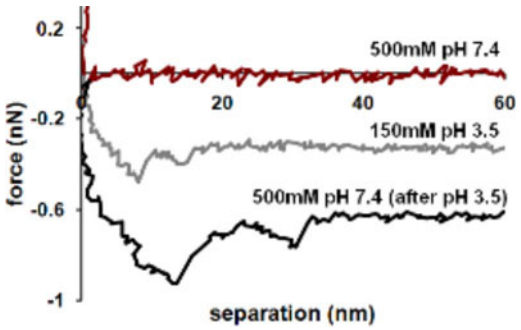

FIG. 8. Force curves collected upon retraction of a fibrinogen coated probe from mica surface first in 500 mM PBS at *p*H 7.4, then in 150 mM PBS *p*H 3.5, and back again in 500 mM PBS *p*H 7.4. Fibrinogen adhesion to the mica surface, which disappears after the raise of the ionic strength to 500 mM, is recovered after the *p*H change to 3.5. The curves have been shifted vertically for better display.

As already discussed, the increase of salt concentration to 500 mM resulted in an irreversible disappearance of fibrinogen adhesion to the surface. The only case, where adhesion was found to recover, was after changing the *p*H to 3.5 (Fig. 8). A likely explanation for this is that at this acidic *p*H the protein structure is altered with certain domains becoming exposed or detached. These domains could then adhere to the surface, even when the rest of the protein molecule shrinks in a compact form at high ionic strengths.

Details about fibrinogen structure can be found in Refs. 49 and 50. In brief, fibrinogen consists of two sets of three different polypeptide chains (α, β, and γ), which are intertwined and held together by disulfide bonds. The *N*-terminal regions of the six chains are folded into a globular central *E* domain, whereas the *C*-terminals of the β and γ chains are folded into two pairs of homologous structures, which form the hydrophobic, negatively charged *D* outer domains. The *C*-terminal regions of the α chains extend from the *D* domains and fold back beside the *E* domain. Fibrinogen polymerization into fibrin is catalyzed by thrombin, which removes the fibrinopeptides *A* and *B* from the amino terminal ends of the α and β chains, so that the latter can interact with the γ and β lobes of the *D* domain, respectively. Several authors[5,25] have suggested fibrinogen conformational changes at *p*H 3.5, with the *C*-terminal regions of the α chains being detached from the central *E* domain of the molecule. These αC arms are positively charged[34,51] and, therefore, when they become free from the *E* domain, they may readily interact with the negatively charged mica surface. On the other hand, they may play a crucial role in fibrinogen polymerization into fibrin, since their detachment from the central domain possibly leaves the fibrinopeptides *A* and *B* uncovered. These two effects may combine, driving to clot formation on surfaces. It is not surprising, then, that at *p*H 3.5 aggregates appear on the surface[24] and adsorption is limited by the decrease of the effective protein concentration.

IV. CONCLUSIONS

In this study, we have presented the interaction and detachment forces measured between fibrinogen-modified AFM probes and mica surfaces. The deposition of plasma polymerized poly(acrylic acid) on silica colloid spheres, attached at the end of the cantilever, and the subsequent covalent binding of protein molecules have proved an efficient method for protein immobilization.

The force curves collected when the colloid probe approaches the surface at various ionic strengths at *p*H 7.4 have shown that at the two lower salt concentrations the protein-surface interaction is controlled by the balance between the electrostatic repulsion and the van der Waals attraction. As the ionic strength was increased from 15 to 150 mM the electrostatic repulsion was screened and an attraction up to the contact point occurred. At 500 mM, however, the hydration forces become crucial, shielding the van der Waals attraction. At the same ionic strength, retraction curves revealed that fibrinogen obtains a compact conformation, which prevents it from attaching to the surface.

Concerning the *p*H, stronger attraction of the protein layer to the surface was recorded at *p*H 5.8 and 3.5 compared with the physiological one, mainly because the hydration forces lose their significance at the acidic *p*H's. Detachment force measurements infer that fibrinogen structure probably changes at *p*H 3.5 with the cleavage of the carboxylic ends of the α-chains from the central *E* domain. This conformational change may influence protein adsorption either by initiating aggregation or by enhancing the molecular interaction with negatively charged surfaces. The role of these arms needs further examination. AFM imaging of the *in situ* polymerization of native or αC terminal-deficient fibrinogen molecules could possibly reveal the exact contribution of these ends to the process of fibrin formation.

Using mica as a substrate for the measurements has shown that the biophysical behavior of intact proteins at interfaces can be estimated. Chemical modification of flat surfaces such as mica, silica, or graphite with self assembled monolayers could be the next step to approach a preactive determination of the biocompatibility of biomaterials.

ACKNOWLEDGMENTS

This work was financially supported by "Irakleitos—EPEAEK II Research Programme." The authors acknowledge M. Taylor for the valuable assistance with the colloid probe preparation and M. Zelzer for the scrupulous supervision of the plasma process. M. C. Davies is gratefully acknowledged for kindly hosting TT at the Laboratory of Biophysics and Surface Analysis within the School of Pharmacy, The University of Nottingham, and "COST 537 Action" is acknowledged for her STSM grant.

[1]C. A. Haynes and W. Norde, Colloids Surf., B **2**, 517 (1994).
[2]P. G. Koutsoukos, C. A. Mumme-Young, W. Norde, and J. Lyklema, Colloids Surf. **5**, 93 (1982).
[3]P. Wagner, FEBS Lett. **430**, 112 (1998).
[4]H. P. Erickson and N. A. Carrell, J. Biol. Chem. **258**, 14539 (1983).
[5]Y. I. Verklich, O. V. Gorkun, L. V. Medved, W. Nieuwenhuizen, and J. W. Weisel, J. Biol. Chem. **268**, 13577 (1993).
[6]A. K. Bajpai, Polym. Int. **54**, 304 (2005).
[7]T. J. Su, J. R. Lu, R. K. Thomas, Z. F. Cui, and J. Penfold, J. Colloid Interface Sci. **203**, 419 (1998).

[8]H. Matsumoto, Y. Koyama, and A. Tanioka, J. Colloid Interface Sci. **264**, 82 (2003).
[9]J. L. Ortega-Vinuesa, P. Tengvall, and I. Lundstrom, Thin Solid Films **324**, 257 (1998).
[10]S. O. Vansteenkiste, S. I. Corneillie, E. H. Schacht, X. Chen, M. C. Davies, M. Moens, and L. Van Vaeck, Langmuir **16**, 3330 (2000).
[11]S. Kidoaki, Y. Nakayama, and T. Matsuda, Langmuir **17**, 1080 (2001).
[12]A. Sethuraman, M. Han, R. S. Kane, and G. Belfort, Langmuir **20**, 7779 (2004).
[13]X. Chen, M. C. Davies, C. J. Roberts, S. J. B. Tendler, and P. M. Williams, Langmuir **13**, 4106 (1997).
[14]M. S. Wang, L. B. Palmer, J. D. Schwarz, and A. Razatos, Langmuir **20**, 7753 (2004).
[15]S. Kidoaki and T. Matsuda, Langmuir **15**, 7639 (1999).
[16]H. Zhang, K. E. Bremmell, and R. S. C. Smart, J. Biomed. Mater. Res. **74A**, 59 (2005).
[17]J. J. Valle-Delgado, J. A. Molina-Bolivar, F. Galisteo-Gonzalez, M. J. Galvez-Ruiz, A. Feiler, and M. W. Rutland, J. Phys.: Condens. Matter **16**, S2383 (2004).
[18]J. J. Valle-Delgado, J. A. Molina-Bolivar, F. Galisteo-Gonzalez, M. J. Galvez-Ruiz, A. Feiler, and M. W. Rutland, J. Phys. Chem. B **108**, 5365 (2004).
[19]L. Meagher and H. J. Griesser, Colloids Surf., B **23**, 125 (2002).
[20]S. L. McGurk, R. J. Green, G. H. W. Sanders, M. C. Davies, C. J. Roberts, S. J. B. Tendler, and P. M. Williams, Langmuir **15**, 5136 (1999).
[21]S. Pasche, J. Voros, H. J. Griesser, N. D. Spencer, and M. Textor, J. Phys. Chem. B **109**, 17545 (2005).
[22]D. J. Muller and A. Engel, Biophys. J. **73**, 1633 (1997).
[23]P. Hinterdorfer and Y. F. Dufrene, Nat. Methods **3**, 347 (2006).
[24]T. S. Tsapikouni and Y. F. Missirlis, Colloids Surf., B **57**, 89 (2007).
[25]S. Jung, S. Lim, F. Albertorio, G. Kim, M. C. Gurau, R. D. Yang, M. A. Holden, and P. S. Cremer, J. Am. Chem. Soc. **125**, 12782 (2003).
[26]P. S. Sit and R. E. Marchant, Surf. Sci. **491**, 421 (2001).
[27]E.-L. Florin, M. Rief, H. Lehmann, M. Ludwig, C. Dornmair, V. T. Moy, and H. E. Gaub, Biosens. Bioelectron. **10**, 895 (1995).
[28]C. T. Gibson, D. J. Johnson, C. Anderson, C. Abell, and T. Rayment, Rev. Sci. Instrum. **75**, 565 (2004).
[29]M. R. Alexander, J. D. Whittle, D. Barton, and R. D. Short, J. Mater. Chem. **14**, 408 (2004).
[30]G. T. Hermanson, *Bioconjugated Techniques* (Academic, San Diego, 1996), Part II, Chap. 3.
[31]S. Candan, A. J. Beck, L. O'Toole, and R. D. Short, J. Vac. Sci. Technol. A **16**, 1702 (1998).
[32]D. M. Czajkowsky and Z. Shao, J. Microsc. **211**, 1 (2003).
[33]M. A. Osman, C. Moor, W. R. Caseri, and U. W. Suter, J. Colloid Interface Sci. **209**, 232 (1999).
[34]T. C. Ta, M. T. Sykes, and M. T. McDermott, Langmuir **14**, 2435 (1998).
[35]W. F. Heinz and J. H. Hoh, Biophys. J. **76**, 528 (1999).
[36]O. H. Willemsen, M. M. E. Snel, L. Kuipers, C. G. Figdor, J. Greve, and B. G. D. Grooth, Biophys. J. **76**, 716 (1999).
[37]R. M. Pashley, J. Colloid Interface Sci. **83**, 531 (1981).
[38]D. Leckband and S. Sivasankar, Colloids Surf., B **14**, 83 (1999).
[39]C. R. Hurley and G. J. Leggett, Langmuir **22**, 4179 (2006).
[40]J. N. Israelachvili, *Intermolecular and Surface Forces* (Academic, London, 1992), Chap. 4.
[41]D. J. Muller, D. Fotiadis, S. Scheuring, S. A. Muller, and A. Engel, Biophys. J. **76**, 1101 (1999).
[42]B. Bhushan, *Handbook of Nanotechnology* (Springer, Berlin, 2004), Chap. 15.
[43]B. P. Frank and G. Belfort, J. Membr. Sci. **212**, 205 (2003).
[44]J. Hemmerle, S. M. Altmann, M. Maaloum, J. K. H. Horber, L. Heinrich, J. C. Voegel, and P. Schaaf, Proc. Natl. Acad. Sci. U.S.A. **96**, 6705 (1999).
[45]A. Verma, J. M. Simard, and V. M. Rotello, Langmuir **20**, 4178 (2004).
[46]Y. Roiter, W. Jaeger, and S. Minko, Polymer **47**, 2493 (2006).
[47]D. McCormack, S. L. Carnie, and D. Y. C. Chan, J. Colloid Interface Sci. **169**, 177 (1995).
[48]R. J. Hunter, *Foundations of Colloid Science* (Oxford Science, New York, 1987), Chap. 7.
[49]R. F. Doolittle, Protein Sci. **1**, 1563 (1992).
[50]C. Fuss, J. C. Palmaz, and E. A. Sprague, J. Vasc. Interv. Radiol. **12**, 677 (2001).
[51]K. L. Marchin and C. L. Berrie, Langmuir **19**, 9883 (2003).